

## Material Science and Engineering with Advanced Research

# Experimental and Finite Element Investigation of Welded T-End Connection to Rectangular Hollow Section (RHS) in Pure Tension

Messaoud Saidani

Faculty of Engineering and Computing, Coventry University, United Kingdom

**\*Corresponding Author:** Messaoud Saidani, Faculty of Engineering and Computing, Coventry University, Priory Street, Coventry CV1 5FB, United Kingdom, Tel: ++4476888385; Email: [m.saidani@coventry.ac.uk](mailto:m.saidani@coventry.ac.uk)

**Article Type:** Research, **Submission Date:** 25 March 2015, **Accepted Date:** 23 April 2015, **Published Date:** 8 May 2015.

**Citation:** Messaoud Saidani (2015) Experimental and finite element investigation of welded T-End connection to rectangular hollow section (RHS) in pure tension. *Mater. Sci. Eng. Adv. Res* 1(1): 5-11. doi: <https://doi.org/10.24218/msear.2015.02>.

**Copyright:** © 2015 Messaoud Saidani. This is an open-access article distributed under the terms of the Creative Commons Attribution License, which permits unrestricted use, distribution, and reproduction in any medium, provided the original author and source are credited.

### Abstract

The present paper investigates the behaviour of welded T-end connections to Rectangular Hollow Section (RHS) members in pure tension. A series of tests in the laboratory and finite element modelling were carried out. The experimental programme consisted of testing to failure of a total of 19 specimens with varying parameters, namely the tube size and cap plate thickness. The failure load and modes of failure were recorded for all specimens. Furthermore, strains (stresses) and deflections at different locations in the connection were also recorded and plotted against the applied load. In order to make the testing programme manageable, the cleat plate thickness and size was kept constant for all the tests. From the test results, it became evident that the cap plate thickness was the most important parameter in deciding the joint capacity and associated mode of failure. The test results were compared with the numerical analysis results using the finite element package ANSYS. Some design recommendations are made based on the work undertaken so far and comparison is made with existing design equations.

### Introduction

The excellent properties of structural hollow sections have long been realised [1,2]. It is often said that connections made with hollow sections are complex and expensive to fabricate. In reality they can be made simple and cost-effective in addition to their higher capacity compared with traditional type of connections made with open sections. This is to add to their excellent aesthetic appearance making them the ideal choice in many elegant structures.

Rectangular hollow section (RHS) members are often used as compressive members due to their good buckling stiffness. Often such members are also required, and indeed should be designed, to take also tensile forces. One of the simplest ways to connect tubular members is by cutting the ends and welding together. However, depending on joint configuration and number of members connected, this may result in complex and expensive connections. The alternative would be to connect the members together through some other means. Figure 1 shows types of end connection detail for hollow tubes that are used in practice. One of the most economic solutions is to weld a cap plate to the tube

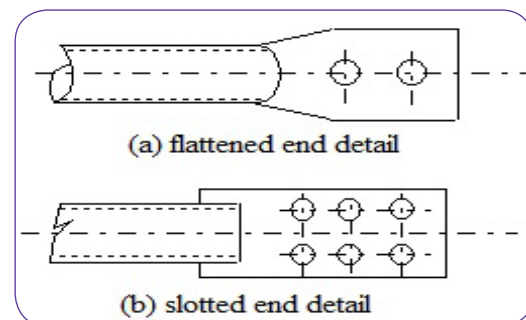


**Figure 1:** Type of end-connections

(CHS or RHS) and then weld on to it a cleat plate (Figure 2). The connection could be made entirely in the workshop, thus reducing labour work on site.

In the UK very little work has been conducted on welded T-end connections. Elsewhere, research work was carried out mainly in Australia [3-5] and Sweden [6]. Such work has also been reported elsewhere [7,8]. Experimental studies conducted by Lehman et al [9] and numerical studies by Yoo et al [10], have clearly indicated that relatively large and thick gusset plate concentrates the cyclic strain demand in the middle of the brace, thereby reducing the deformation capacity of the brace. Uriz et al [11], presented a model for the inelastic buckling behaviour of steel braces. The model consisted of a force-based frame element with distributed inelasticity and fiber discretization of the cross section. Even though the model does not account for the effect of local buckling, this phenomenon does not seem to appreciably affect the global response of braces with compact sections.

Nascimbene [12] proposed non-standard numerical modelling of thin-shell structures through geometrically linear formulation. A two dimensional, three- and five-node arch element was developed devoid of shear and membrane locking, even in the extreme thin limit. By adopting different choices on the shape functions regarding shear, bending, and membrane strains appropriately projected over Gauss integration points, a family of locking free-shell finite elements were derived. The undesired locking phenomena were completely suppressed. A range of numerical examples were given by the author to show the accuracy of the formulation proposed and comparisons with well-known shell finite elements.

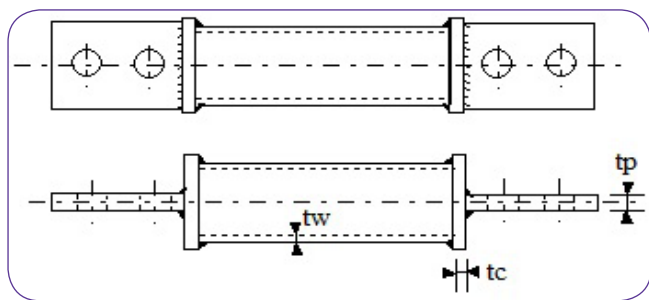


Figure 2: Welded T-end plate connection

For bracing connections, the absence of design recommendation very often leads designers to specify uneconomical solutions, as is shown in Figure 2.

Research has shown that welded T-end connections subjected to uniform tension may fail in different ways. The failure mode is dictated by parameters such as tube wall thickness  $t_w$ , cap plate thickness  $t_c$ , cleat plate thickness  $t_p$ , and weld size and quality. The possible resulting modes of failure are as follows:

- (a) Tube yielding;
- (b) Local fracture in tube (in the region adjacent to weld);
- (c) Fracture of the weld;
- (d) Yielding of the cap plate;
- (e) Shear failure of the cap plate;
- (f) Yielding of the cleat plate.

Combination of more than one mode of failure is possible. In a truss environment (when the connection forms part of the truss assembly), there is also the possibility of the bolts failing.

The problem being investigated in this research programme is to answer the fundamental question: how does the cap plate thickness influence the mode(s) of failure of the connection? In order to answer this question, an experimental programme was conducted on a series of specimens with varying parameters.

### Experimental Programme

The experimental programme followed a similar procedure adopted in a previous study [4] show that useful comparison could be made. The testing work included 19 specimens with varying tube wall and cap plate thickness. Each specimen was loaded in tension, taking all precautions to avoid any accidental eccentricity. Strains and deformations were also measured. The test arrangement for the strain gauges and LVDT's is shown in Figure 3 (illustration shown for specimen number 1). The programme of tests is summarised in Table 1. In order to keep the investigation manageable, only one cleat plate thickness was used and kept equal to 15mm for all specimens. Combination of square and true rectangular hollow section tubes, were used. In specimens 12, 13, 14, and 15, the cleat plate is parallel to the longer side of the tube, whereas in specimens 16, 17, 18, and 19, the cleat plate is parallel to shorter side of the tube.

The test programme was devised to concentrate on the yielding of the tube wall and the deformation of the cap plate as these were found to be the main causes of failure. Strain gauges were located on the tube wall (four faces), the cap plate, and the cleat plate with the aim of closely monitoring strain (and stress) variations across the specimen. The LVDT's will give readings of the deformations and an indication of any in-plane and/or out-of-plane movements.

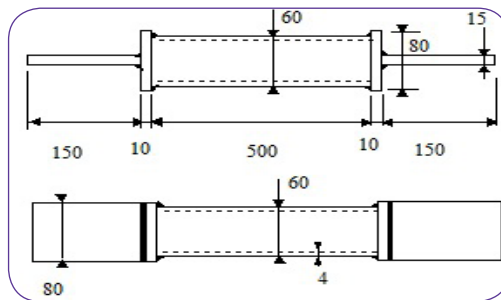


Figure 3: Dimensions for specimen number 1

It is important that the strain gauges are kept far enough from welds in order to avoid any influence from the residual stresses on the readings. The total length of the tube is 500mm again for the same reason. Strain gauges were placed on opposite sides so that in-plane and out-plane bending moments could be monitored and calculated. The general arrangement for the testing is shown in Figure 4. In total 16 strain gauges and 5 LVDT devices were used to monitor the joint behaviour and obtain the necessary information.

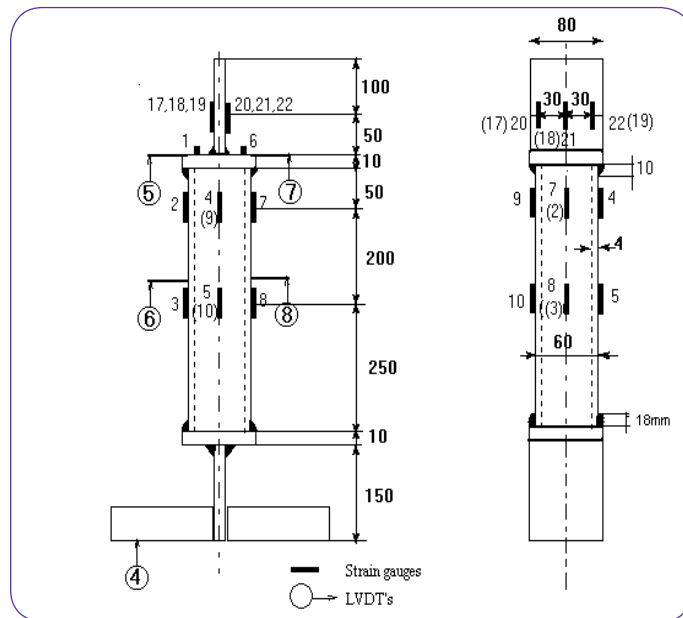


Figure 4: Joint testing arrangement

All tubes used for making the specimens were obtained from Corus. Samples were cut out from each specimen and were tested in accordance with British Standards for testing in order to check the material properties (Young's modulus, yield strength, and ultimate tensile strength). Accurate material properties are important to obtain since these are needed for accurate numerical modelling of the specimens as described in section 4 (finite element modelling).

### Specimens Testing and Results

The DENISON machine with a capacity of 500kN was used for the testing of the joints. The tensile load was applied in increments of 10kN up to failure. The strains and deformations were recorded for each load increment into a computer logged to the testing machine. Using a simple spreadsheet program, stresses were calculated and various graphs were plotted.

Table 2 summarises the results from the specimen testing. For test No.1, the failure was due to weld fracture. On close examination of the specimen it was discovered that weld penetration was not adequate. As a result, it was decided that welding should be done

Test number	Tube properties				Cleat Plate		Cap Plate	
	Nominal Dimensions		Area $A_{tw}$ (mm <sup>2</sup> )	Yield stress $\sigma_{yw}$ (Mpa)	Ultimate Stress $\sigma_{uw}$ (Mpa)	$t_p$ (mm)	Area (mm <sup>2</sup> )	$t_c$ (mm)
	$B_w \times D_w$ (mm)	$t_w$ (mm)						
1	60 × 60	4	879	390.6	514.37	15	1200	10
2	60 × 60	4	879	390.6	514.37	15	1200	10
3	60 × 60	4	879	390.6	514.37	15	1200	15
4	60 × 60	4	879	390.6	514.37	15	1200	20
5	60 × 60	4	879	390.6	514.37	15	1200	25
6	60 × 60	4	879	390.6	514.37	15	1200	26
7	60 × 60	4	879	390.6	514.37	15	1200	28
8	60 × 60	4	879	390.6	514.37	15	1200	30
9	80 × 80	3.6	1090	414.6	523	15	1500	20
10	80 × 80	3.6	1090	414.6	523	15	1500	15
11	80 × 80	3.6	1090	414.6	523	15	1500	20
12	60 × 40	4	719	350	517	15	1200	10
13	60 × 40	4	719	350	517	15	1200	15
14	80 × 40	3.2	716	355	540	15	1500	10
15	80 × 40	3.2	716	355	540	15	1500	15
16	40 × 60	4	719	350	517	15	900	10
17	40 × 60	4	719	350	517	15	900	15
18	40 × 80	3.2	716	355	540	15	900	10
19	40 × 80	3.2	716	355	540	15	900	15

**Table 1:** Testing programme

very carefully making sure it is evenly spread with sufficient material penetration. In the subsequent specimens, failure was mainly due to generalised tube yielding. Yielding was also noticeable in the cap plate.

In all the tests, the determination of the first yield point was proven very difficult to do accurately. The values shown in Table 2 were obtained by considering the load-axial deflection curve and taking the point where departure from the initial elastic path became measurable. The load-stress curves were also used to help with the determination of the first yield point. Figures 5 and Figure 6 show typical load-deformation and load-strain curves for specimen No.2.

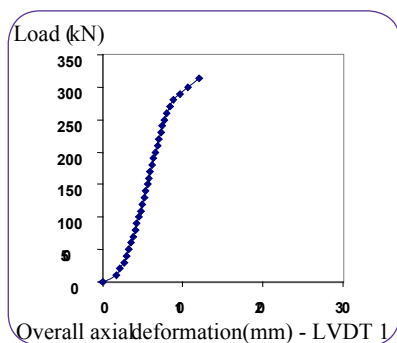


**Figure 5:** Load vs axial deformation

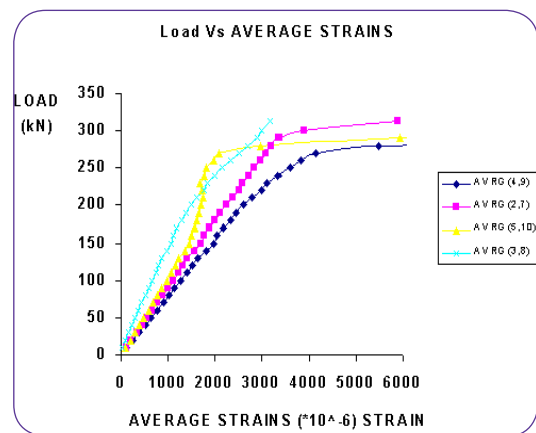


**Figure 6:** Load vs strain (SG/3)

Using the strain gauge readings, in-plane and out-of-plane bending moments were calculated in order to check their relative significance. Again, typically, results for specimen No.2 are shown in Figures 7 and Figure 8 respectively.

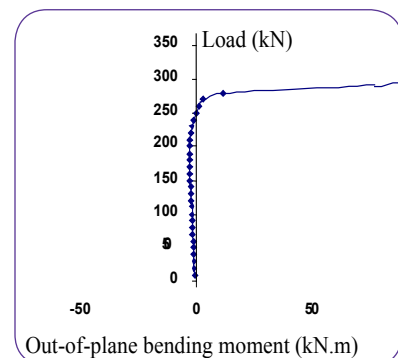


**Figure 7:** Load vs out-of-plane bending

Test Designation	Experimental Loads			Failure Mode
	P <sub>FY</sub> (kN)	P <sub>UE</sub> (kN)	P <sub>UE</sub> /P <sub>FY</sub>	
1	190	240	1.26	Weld Fracture
2	230	280	1.22	Local Tube yielding & hinges in cap plate
3	265	300	1.13	Generalised tube yielding
4	280	320	1.14	Generalised tube yielding
5	300	350	1.16	Generalised tube yielding
6	290	330	1.14	Generalised tube yielding
7	220	320	1.45	Generalised tube yielding
8	230	310	1.35	Generalised tube yielding
9	230	330	1.43	Local fracture
10	320	420	1.31	Generalised tube yielding
11	370	450	1.21	Generalised tube yielding
12	240	300	1.25	Local fracture
13	260	330	1.27	Generalised tube yielding
14	170	240	1.41	Local Fracture
15	190	260	1.37	Generalised tube yielding
16	200	280	1.4	Generalised tube yielding
17	230	300	1.3	Generalised tube yielding
18	150	230	1.53	Generalised tube yielding
19	160	240	1.5	Generalised tube yielding

Table 2: Summary of the testing results

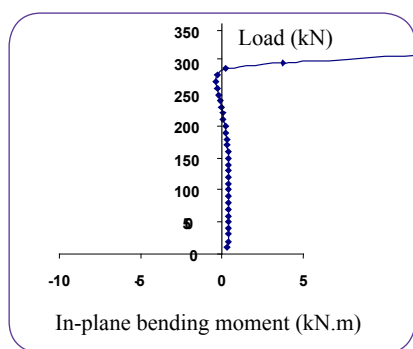


Figure 8: Load vs in-plane bending

As can be seen from Table 2, for a given tube size, both the ultimate loads and observed first yield loads increase with the cap plate thickness. However, this trend was reversed when the cap plate thickness reaches about 25 mm, when the joint capacity (ultimate load) started to decrease with increased cap plate thickness (see Table 2). This was a surprising observation. The test for the 25mm cap plate thickness was repeated three times (although not clear from the Table) since there were some doubts about the results, and every time the results were almost the same. This seems to suggest that, as the cap plate thickness increases beyond 25mm, the ultimate capacity of the connection decrease (existence of an optimum value for the cap plate thickness). This could be explained by the fact that, as the cap plate becomes very thick, the tube would yield earlier resulting in a reduction in the joint capacity.

For joints to a true RHS tube, as can be seen from Table 2, the orientation of the cleat plate relative to the tube seems to affect the joint capacity. In cases where the cleat plate is parallel to longer side of the tube, then the capacity of the joint is bigger than the case when the cleat plate is parallel to the shorter side of the tube (compare specimen 12,13 with 16,17 and specimen 14,15 with 18,19, respectively). Therefore, from a practical viewpoint, it is more efficient to always weld the cleat plate parallel to the longer side of the tube in order to achieve a higher joint strength. It is also evident from Figure 6 that extensive stress redistribution was taking place.

Examination of Figure 7 and Figure 8 show that the in-plane and out-of-plane bending moments were small and could be therefore ignored. As the load approaches the failure load, the deformations in the specimen become more important resulting in a sharp increase in in-plane and out-of-plane bending moments. Again, this was characteristic in all the joints tested.

Three particular modes of failure were observed: (a) weld fracture; (b) tube yield failure; (c) local fracture of the tube wall at the vicinity of the weld. Failure mode (a) would only occur if the weld were the weakest part of the joint. This could be avoided by carefully controlling the quality (and size) of the weld. Failure mode (b) is the more general one, occurring in almost all the tests. If the welds in the cap plate-tube connection and the cleat plate-tube connection are strong, then failure mode (c) may take place especially for connections with thinner plates. As can be seen from Figure 5, the axial deformation remains linear for load of up to 230kN (estimated first yield point). In this case, the failure load was 313kN. This gives a ratio of ultimate strength to yield strength of 1.36. In reality the ultimate load could be higher

since the test was stopped as soon as the machine ceased taking any more loads. The strains at mid-height of the tube (Figure 6) were linear up to about 150kN and thereafter non-linear. This was typical in all the specimens tested.

### Finite Element Modelling and Analysis

The finite element (FE) analysis of the specimens was undertaken using a FE package [13]. Because of symmetry, only half of the specimen was modelled (it was also possible to model only one eighth of the specimen although it was not done). The joint and the welds were modelled using solid elements (see Figure 9 for FE mesh). 3-D, 4 node tetrahedral structural solid elements 'SOLID 72' with three translational, three rotational degrees of freedom (DOF) per node, and defined by six degrees of freedom at each node, were chosen. The tensile load was applied as a uniformly distributed load at the end of the cleat plate. The model developed by the author using ANSYS was free from the locking phenomena and spurious energy mode as identified by other researchers stated above.

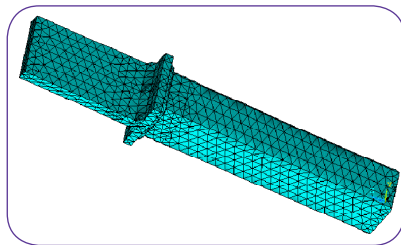


**Figure 9:** Finite element mesh for half a joint

Figure 10 show the strain distribution in the tube wall in the vicinity of the weld using averages of SG's on opposite sides of the tube wall (see Figure 1 for SG's location). It can be seen that reasonably good agreement exists between the test results and the FE results, especially in the linear elastic range. There is still room for improving the FE model by including the real material properties of the weld and also by appropriate choice of weld FE elements.

In Table 3 are listed the values of the failure loads for each specimen obtained from the test results and the FE analysis. The failure load from the FE analysis was obtained by using deformation criteria. The deformation obtained at failure for each specimen was used as the failure criteria and incorporated in the FE analysis. Strain criteria could also have been used, but the results should not differ by too much since deformations and strains are related. A more accurate approach would be to use the ultimate strains obtained from the material property of the specimens. In any case, it can be seen from Table 3 that agreement between the FE and test results is very good with a maximum difference of 7%. It can also be seen from Table 3 that the FE analysis confirmed previous finding from the experimental work concerning the effects of the cap plate thickness and the orientation of the cleat plate relative to the tube on the capacity of the joint.

Results of ultimate load obtained from yield line failure models previously developed [4] are also shown in Table 3 for comparison. Overall, the yield line method seems to give a good prediction of joint capacity. However, for connections with thinner cap plate, the predicted values are not always on the safe side. Also, the method does not accommodate the fact that for connections

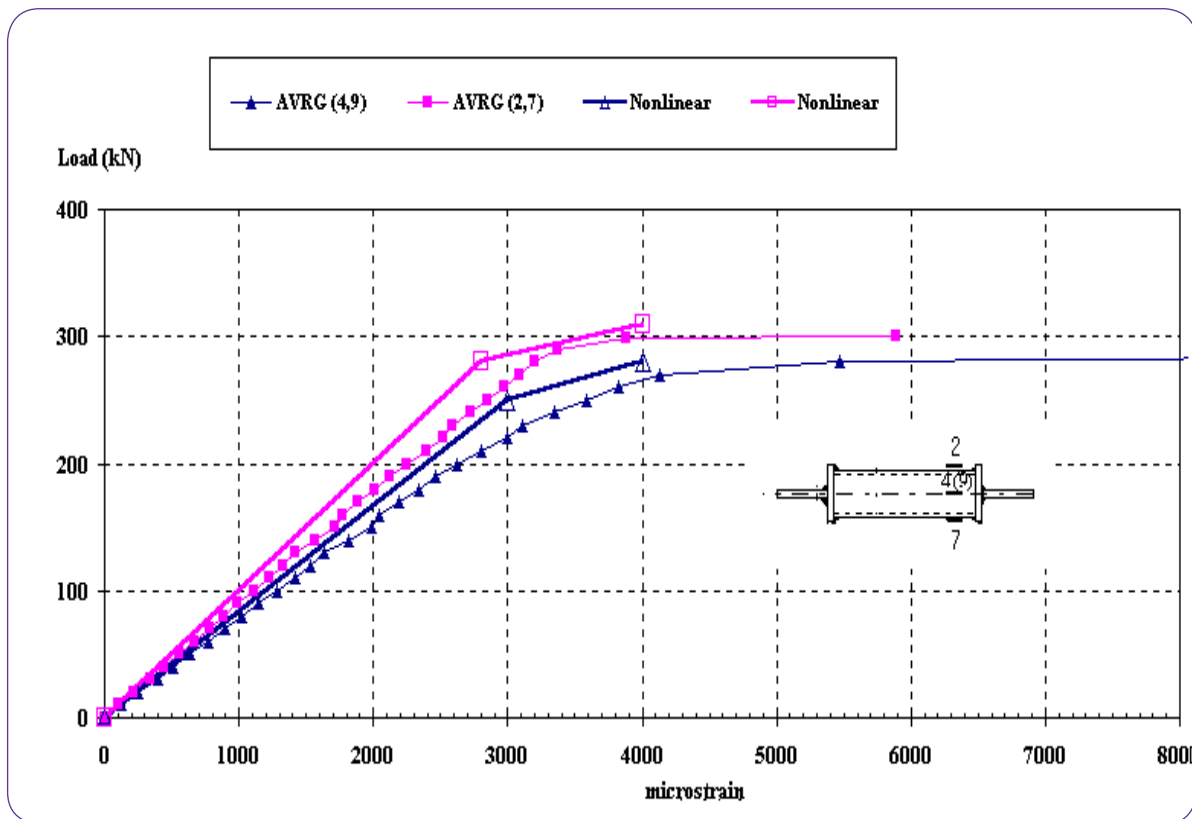


**Figure 10:** Average strains from test and FE results

Test number	Tube size (mm)	cap plate $t_c$ (mm)	Failure load (Tests) $P_{ue}$ (kN)	Predicted failure load (FE) $P_{FE}$ (kN)	Predicted failure load from yield line mechanisms* (kN)	$P_{ue}/P_{FE}$
1	60x60x4	10	260	280	343.34	0.93
2	60x60x4	10	280	280	343.34	1.00
3	60x60x4	15	300	308	343.34	0.97
4	60x60x4	20	320	320	343.34	1.00
5	60x60x4	25	350	346	343.34	1.01
6	60x60x4	26	330	339	343.34	0.97
7	60x60x4	28	320	318	343.34	1.01
8	60x60x4	30	310	318	343.34	0.97
9	80x80x3.6	10	330	329	308.87	1.00
10	80x80x3.6	15	420	420	420.33	1.00
11	80x80x3.6	20	450	460	451.91	0.98
12	60x40x4	10	300	284	251.65	1.06
13	60x40x4	15	330	336	251.65	0.98
14	80x40x3.2	10	240	253	254.18	0.95
15	80x40x3.2	15	260	271	254.18	0.96
16	40x60x4	10	280	286	251.65	0.98
17	40x60x4	15	300	295	251.65	1.02
18	40x80x3.2	10	230	226	207.84	1.02
19	40x80x3.2	15	240	235	254.18	1.02

**Table 3:** Failure loads from experimental, FE results, and Yield line models\*  
\* (Stevens & Kitipornchai 1990)

with thick cap plate, the joint capacity is reduced.

## Conclusions and Future Work

The behaviour of welded T-end connections has been investigated through a series of tests. Numerical models have also been used to predict their behaviour. It was found that, apart from any weld defects, the mode of failure of the joint could be by generalised tube yielding or local fracture of the tube wall.

It was also found that, for a given tube size, the joint capacity increases with increased cap plate thickness. However, the existence of an optimum value for the cap plate was found. Both the FE and test results have shown that as the cap plate become very thick (more than about 25mm), the capacity of the joint started to decrease with increased cap plate thickness, suggesting that joints with excessively thicker plates are less stronger than would normally be expected. The results also suggest that considerable stress re-distribution and strain hardening were taking place after the first yield. The effect of changing the orientation of the cap plate in relation to the tube was also examined. It was found that, in joints with true RHS, it is more efficient to place the cleat plate parallel to the longer side of the tube. The FE results agree reasonably well with the test results, but there is room for further improvement of the FE model by careful modelling of the welds.

## References

- Cran JA. Worldwide applications of structural hollow sections; the sky's the limit. Symposium on tubular structures; 1977; Delft, The Netherlands. 23.1-23.14.
- Comite International pour le Developpement et l'Etude de la Construction Tubulaire, British Steel, and the Commission of the European Communities 1984. Construction with hollow sections, Wellingborough, Northants, UK.
- Kitipornchai S, Traves WH. Welded T-end connections for circular hollow tubes. Journal of Structural Engineering (ASCE). 1989; 115(12):3155-3170. doi: [http://dx.doi.org/10.1061/\(ASCE\)0733-9445\(1989\)115:12\(3155\)](http://dx.doi.org/10.1061/(ASCE)0733-9445(1989)115:12(3155)).
- Stevens NJ, Kitipornchai S. Limit analysis of welded tee end connections for hollow tubes. Journal of Structural Engineering (ASCE). 1990; 116(9):2309-2323. doi: [http://dx.doi.org/10.1061/\(ASCE\)0733-9445\(1990\)116:9\(2309\)](http://dx.doi.org/10.1061/(ASCE)0733-9445(1990)116:9(2309)).
- Zhao XL, Hancock GJ. T-Joints in rectangular hollow sections subject to combined actions. Journal of Structural Engineering (ASCE). 1991; 117(8):2258-2277. doi: [http://dx.doi.org/10.1061/\(ASCE\)0733-9445\(1991\)117:8\(2258\)](http://dx.doi.org/10.1061/(ASCE)0733-9445(1991)117:8(2258)).
- Granstrom A. End plate connections for rectangular hollow sections. Sweden: Stålbyggnadsinst (SBI); 1979.
- Packer JA, Henderson JE. Hollow Structural Section. Connections and Trusses. 2<sup>nd</sup> ed. Canada: Canadian Institute of Steel Constructors; 1997.
- Syam AA, Chapman BG. Design of structural steel hollow section connections. 1<sup>st</sup> ed. North Sydney: Australian Institute of Steel Construction. 1997.
- Lehman DE, Roeder CW, Herman D, Johnson S, Kotulka B. Improved Seismic Performance of Gusset Plate Connections. Journal of Structural Engineering (ASCE). 2008; 134(6):890-901. doi: [http://dx.doi.org/10.1061/\(ASCE\)0733-9445\(2008\)134:6\(890\)](http://dx.doi.org/10.1061/(ASCE)0733-9445(2008)134:6(890)).
- Yoo JH, Lehman DE, Roeder CW. Influence of connection design parameter on the seismic performance of braced frames. Journal of Constructional Steel Research. 2008; 64(6):608-622. doi: [10.1016/j.jcsr.2007.11.005](https://doi.org/10.1016/j.jcsr.2007.11.005).
- Uriz P, Filippou FC, Mahin SA. Model for cyclic inelastic buckling for steel member. Journal of Structural Engineering (ASCE). 2008; 134(4):616-628. doi: [http://dx.doi.org/10.1061/\(ASCE\)0733-9445\(2008\)134:4\(619\)](http://dx.doi.org/10.1061/(ASCE)0733-9445(2008)134:4(619)).

12. Nascimbene R. Towards Non-Standard Numerical Modelling of Thin-Shell Structures: Geometrically Linear Formulation. International Journal for Computational Mechanics in Engineering Science and Mechanics. 2014;15(2):126-141.doi:10.1080/15502287.2013.874058.
13. ANSYS. Engineering Analysis System User Manual. Houston, PA: Swanson Analysis Systems Inc. 2013.